Scattering of light in a Bose Einstein condensate

Ayush Goyal

2021

1 INTRODUCTION

1.1 Scattering of light

When light passes through any medium, we observe that the light interacts with the particles of the medium and the deviation of light due to this interaction is termed as the scattering of light. This fundamental process has attracted a lot of scientists across the centuries and thus have been explained in a variety of theories to understand the underlying light matter interactions. To study this behaviour, Max Planck modeled the blackbody radiation in 1899 and Albert Einstein published his theory about the photoelectric effect where light is quantized. The scattering of light can be studied by the light matter interactions, which was explained by Lord Rayleigh in 1871 as the quasi elastic scattering of light for the interaction of light with particles that have their size comparable to the wavelength of light. Later on, C.V. Raman formulated the theory of Raman scattering in 1922 to explain the inelastic interaction of light and matter (i.e. exchange of energy) and the effect put together is explained by the Stokes and Anti-Stokes equations.

Since light behaves as a wave as well as a particle, the optical field representation depends on the experiment and thus the nature of light -matter interactions depend on the behaviour of light in that experiment. Consequently, the scattering of light is a feature dependent on the interaction as particle or wave macroscopically, and on the frequencies and phase differences involved.

In light matter interactions at the microscopic scale, we are concerned interactions behave differently and we thus use semiclassical or quantum properties to describe the nature of light in these interactions. Here the wavelength of light and the size of atom are comparable, and we are concerned with the Rayleigh, Raman or Bragg scattering. Moreover, our area of interest extends to the atomic population and coherences, the optical field

evolution and the atomic motion due to the optical forces. This gives rise to the study of the light behaviour as well as the atom behaviour that is caused by the interactions that may lead to entanglements between photons, atoms and Bose Einstein condensates.

1.2 Bose – Einstein Condensate

A Bose Einstein condensate is a peculiar state of matter which is produced by super cooling a gas of bosons (elementary particles with integer spin governed by Bose-Einstein statistics, e.g. photon gas, ensemble of Helium 4 atoms) with low density at temperatures close to absolute zero, so that all the bosons occupy the same ground state. Here, since most bosons occupy the lowest quantum state there is observance of microscopic quantum phenomenon macroscopically. Interestingly, a BEC consists of non-interacting particles with no apparent internal degrees of freedom which are cooled below the critical temperature.

$$T_c = (\frac{n}{\zeta(3/2)})^{2/3}\frac{2\pi\hbar^2}{mk_B} \approx 3.3125\frac{\hbar^2 n^{2/3}}{mk_B}$$

Where n is the particle density, m is the mass per boson, $\hbar$ is the reduced Planck constant, k_B is the Boltzmann constant and ζ is the Riemann zeta function($\zeta(3/2) \approx 2.6124$) Quantum mechanically, the energy of the condensed particles for the condensate wavefunction $\psi(\vec{r})$ can be represented as

$$E = \int d\vec{r}[\frac{\hbar^2}{2m}|\nabla\psi(\vec{r})|^2 + V(\vec{r})|\psi(\vec{r})|^2 + \frac{1}{2}U_0|\psi(\vec{r})|^4]$$

which is just the non-linear Schrodinger equation for energy minimization.

2 Basic Light Matter Interactions

To study the scattering of light in a Bose-Einstein Einstein, we need to know the light matter interations for a basic 2-level atom and form the basis of the interactions involved. Thus, we first take into consideration a 2-level atom and a constant optical field.

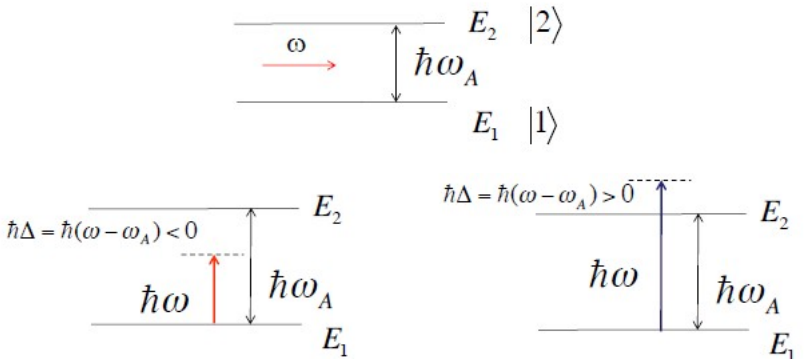

We know that an atom behaves as a quantum harmonic oscillator with quantized energy levels and Hamiltonians of the atom and its interaction with a constant electric field can be represented as:

$$i\hbar\frac{\partial}{\partial t}|\psi\rangle = (H_0 + H_I)|\psi\rangle = (\sum_{i=1}^{2} E_i a_i^+ a_i + \hbar g[a_1^+ a_2 e^{i\omega t} + a_2^+ a_1 e^{-i\omega t}])|\psi\rangle$$

$$i\hbar\begin{pmatrix}\dot{\alpha_1}|1\rangle \\ \dot{\alpha_2}|2\rangle\end{pmatrix} = \begin{pmatrix}E_1 & \hbar g e^{i\omega t} \\ \hbar g e^{-i\omega t} & E_2\end{pmatrix}\begin{pmatrix}\alpha_1|1\rangle \\ \alpha_2|2\rangle\end{pmatrix}$$

For the representation of this state without the dependence on H_0 i.e. the internal atomic properties (we use unitary operation $|\psi_I\rangle = U(t)|\psi_s\rangle = e^{iH_0 t/\hbar}|\psi_s\rangle$), the Schrödinger equation can be represented as

$$i\hbar\frac{\partial}{\partial t}|\psi_I\rangle = \hat{H_I}|\psi_I\rangle = \hbar g(a_1^+ a_2 e^{i\Delta t} + a_2^+ a_1 e^{-i\Delta t})|\psi_I\rangle$$

where $\Delta = \omega - \omega_A$ is the detuning by unitary representation of the state function

which in turn is represented in terms of the density operator by

$$\frac{\partial}{\partial t}\rho = -\frac{i}{\hbar}[H_I, \rho]$$

where $H_I = \hbar g(a_1^+ a_2 e^{i\Delta t} + a_2^+ a_1 e^{-i\Delta t})$; $|\psi\rangle = \sum_i \alpha_i(t)|i\rangle$

Thus, all the interactions can be represented in Matrix form

$$\begin{pmatrix}\dot{\rho_{11}} & \dot{\rho_{12}} \\ \dot{\rho_{21}} & \dot{\rho_{22}}\end{pmatrix} = -\frac{i}{\hbar}[H_I, \rho] = -ig\left[\begin{pmatrix}\rho_{21}e^{i\Delta t} & \rho_{22}e^{i\Delta t} \\ \rho_{11}e^{-i\Delta t} & \rho_{12}e^{-i\Delta t}\end{pmatrix} - \begin{pmatrix}\rho_{12}e^{i\Delta t} & \rho_{11}e^{i\Delta t} \\ \rho_{22}e^{-i\Delta t} & \rho_{21}e^{-i\Delta t}\end{pmatrix}\right]$$

which gives the reversible Bloch equations by removing explicit time dependence:

$$\frac{dR_{11}}{dt} = -ig(R_{21} - R_{12}) \tag{1}$$

$$\frac{dR_{22}}{dt} = -ig(R_{12} - R_{21}) \tag{2}$$

$$\frac{dR_{12}}{dt} = -ig(R_{22} - R_{11}) - i\Delta R_{12} \tag{3}$$

$$\frac{dR_{21}}{dt} = -ig(R_{11} - R_{22}) - i\Delta R_{21} \tag{4}$$

$\Delta = \omega - \omega_0$, $g = \frac{\mu_{12}E}{2\hbar}$ are the detuning and Rabi frequency respectively; $R_{11} = \rho_{11}, R_{22} = \rho_{22}, R_{12} = \rho_{12}e^{-i\Delta t}, R_{21} = \rho_{21}e^{i\Delta t}$ are the populations and coherences respectively.

Defining the difference variable as $D = \frac{R_{22} - R_{11}}{2}$, we get

$$\frac{dD}{dt} = -ig(R_{12} - R_{21})$$

$$\frac{dR_{12}}{dt} = -2igD - i\Delta R_{12}$$

These equations satisfy the conservation relation:

$$D^2 + Re(R_{12})^2 + Im(R_{12})^2 = \frac{1}{4}$$

This gives a simple Bloch sphere and the vector rotates in a circle with Rabi oscillation for a given Δ.

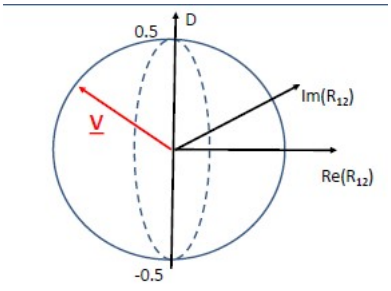

Physically, this represents the system where the atom goes from ground state to excitated state and back to ground state (or vice versa) and amplitude is dependent on the detuning (maximum for resonant case); and photons are

being absorbed and stimulatedly emitted repeatedly giving us an atom with superposition of ground and excited state.

Now, adding a little complexity to the model, we take into consideration an evolving optical field driven by the polarisation described by maxwell's wave equations giving rise to:

$$(\frac{\partial^2}{\partial z^2} - \frac{1}{c^2}\frac{\partial^2}{\partial t^2})\underline{E} = \mu_0 \frac{\partial^2 \underline{P}}{\partial t^2}$$

Assuming $\Delta = 0$ for resonant case, no external input field and only a single cavity mode, the cavity field can be described by

$$\frac{dE(t)}{dt} = -\kappa E + C n_a R_{12}$$

which gives us the time dependent Rabi frequency G(t) as,

$$\frac{dG(t)}{dt} = -\kappa G + i g_0^2 N R_{12}$$

where $g_0 = \mu_{12}\sqrt{\frac{\omega}{2\hbar\epsilon_0 V}}$ is the single photon Rabi frequency

This is the damped pendulum equation for $G(t) = \frac{1}{2}\frac{d\theta(t)}{dt}$ where θ is the angle for the Block vector motion. For the case of weak damping i.e. good cavity, we get the same oscillating equation but for strong damping, $\kappa \gg \sqrt{g_0^2 N}$ i.e. bad cavity, the optical field grows as

$$G(t) \propto e^{(\frac{t}{\tau_R})} = e^{(\frac{N g_0^2}{\kappa} t)}$$

, and N atoms are emitting energy $N\hbar\omega_a \propto N$ in a time $\tau_R \propto \frac{1}{N}$, thus the intensity varies as $P \propto \frac{N}{\frac{1}{N}} \propto N^2$

Here, N atoms emit radiation as a pulse whose duration increases with N and peak power increases as N^2, which was termed as **superradiance** by Dicke(in one of the foundational papers for quantum optics) in 1953 [3], where he approximated a gas of atoms as dipoles and quantum mechanically found the radiative pulse valid for all temperatures and for excitation of states $m \sim 0$ to be

$$I = \frac{1}{4} I_0 N(N-1) tanh^2(E/2kT) + \frac{1}{2} N I_0$$

where intensity is proportional to N^2. This was first observed in 1973 in MIT [13] by detecting superradiance in optically pumped HF gas by an intense short pulse HF laser at 1 mTorr pressure and came to a conclusion that

a superradiant pulse can evolve in an inhomogeneous broadened extended sample where high gain counteracts the dephasing giving rise to effective dephasing time which is much longer than the pulse evolution time and thus, the time scale of the pulse evolution depends on the total number of excited molecules, irrespective of the extend of inhomogeneous broadening.

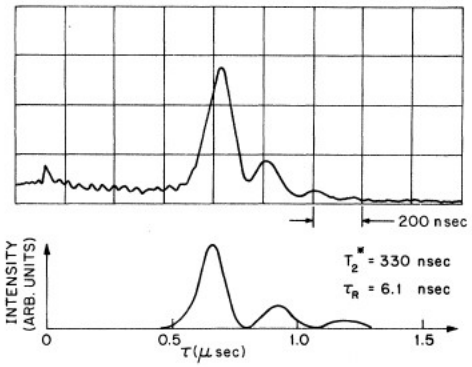

FIG. 1. Oscilloscope trace of superradiant pulse at 84 μm ($J=3\rightarrow 2$), pumped by the $R_1(2)$ laser line, and theoretical fit. The parameters are $I=1$ kW/cm^2, $p=1.3$ mTorr, and $kl=2.5$ for $l=100$ cm. The small peak on the scope trace at $\tau=0$ is the 3-μm pump pulse, highly attenuated.

3 Cold Atoms

Before discussing scattering in cold atoms, we include the damping due to spontaneous emission for atomic dynamics and thus our Bloch equations become

$$\frac{dR_{11}}{dt} = -ig(R_{21} - R_{12}) + 2\gamma R_{22} \tag{5}$$

$$\frac{dR_{22}}{dt} = -ig(R_{12} - R_{21}) - 2\gamma R_{22} \tag{6}$$

$$\frac{dR_{12}}{dt} = -ig(R_{22} - R_{11}) - i\Delta R_{12} - \gamma R_{12} \tag{7}$$

$$\Delta = \omega - \omega_0$$

$$g = \frac{\mu_{12} E}{2\hbar}$$

γ is the coherence damping rate and 2γ is the population damping rate.

Now since we consider cold atoms $R_{11} \approx 1$ and $R_{22} \approx 0$ we get

$$\frac{dR_{12}}{dt} = +ig - i\Delta R_{12} - \gamma R_{12} \text{ assuming } g^2 \ll \gamma^2 + \Delta^2$$

where atoms behave as linear dipoles ($R_{12} = \alpha E$ and polarizability $\alpha = \frac{\mu_{12}}{2\hbar(\Delta - i\gamma)}$).

Also, we calculate microscopic polarization using Dirac delta function as $\underline{P} = \sum_{j=1}^{N} \underline{d}_j \delta(\underline{r} - \underline{r}_j)$ implying $\overline{P} = \frac{1}{V} \sum_{j=1}^{N} \underline{d}_j = \frac{N}{V} \langle \underline{d} \rangle$ and since the atoms behave as linear dipoles, our optical field evolution becomes

$$\frac{dE_{scat}(t)}{dt} = -\kappa E_{scat} + cn_a(E_{pump}\langle e^{-2ikz} \rangle + E_{scat}) \text{ ,thus}$$

$$\underline{P} \Rightarrow \frac{dE_{scat}(t)}{dt} \propto NE_{pump}\langle e^{-2ikz} \rangle$$

We observe that the scattered field depends on the spatial distribution of the atoms and for random atomic positions, $\langle e^{-2ikz} \rangle$ is independent of N giving normal elastic Rayleigh scattering.

The optical force on an atom based on the interaction energy for a linear dipole can be described as

$$F_z = (\alpha \underline{E}(z = z_j)) \cdot \frac{\partial \underline{E}}{\partial z}$$

thus

$$F_z \propto (E_{pump} E_{scat} e^{2ikz} + c.c.)$$

Thus the equations to explain cold atoms become

$$\frac{dz_j}{dt} = \frac{p_j}{m}$$

$$\frac{dp_j}{dt} = -2\hbar k g_p (a e^{2ikz_j} + c.c.)$$

$$\frac{da}{dt} = g_p N \langle e^{-2ikz} \rangle - \kappa a + i\delta a$$

where
$g_p = (\frac{\Omega_p}{\Delta}) g_0$ is a coupling constant which includes the pump amplitude
$|a|^2 = \frac{\frac{1}{2}\epsilon_0 |E|^2 V}{\hbar\omega}$ is the number of photons in the interaction volume V
$\delta = \omega_p - \omega_s$ is the detuning between the pump and scattered fields

From these equations, we have an unstable stationary state where $\langle e^{-2ikz} \rangle = 0$, $p_j = 0$ and $a = 0$ and the scattered intensity and the density modulation grow $\propto e^{\lambda t}$ and maximum growth rate occurs at $\delta = 0$ i.e. $\omega_s \approx \omega_p$ (resonance) and that the rate $Re(\lambda) \propto N^{1/3}$ with $I_{scat} \propto N^{4/3} or N^2$ depending on the size of damping factor κ.

We understand that this behavaviour gives rise to a collective elastic Rayleigh scattering experiment and is termed as Collective Atomic Recoil lasing where there is exponential amplification of the scattered field, with simultaneous periodic atomic density modulation due to the spontaneous ordering of cold atoms by global coupling of light, and the type of cavity determines the different scattered intensity evolutions.

This behaviour was observed in Eberhard-Karls-Universität Tubingen in 2007[14] where superradiant Rayleigh scattering is observed due to collective atomic recoil lasing in a ring cavity and, bad cavity and good cavity characteristics were both measured.They produced a cloud of ultracold ^{87}Rb in a magnetic trap and then moved the cloud into the mode volume of a high finesse optical ring cavity where the atoms move from a 2D magneto-optical trap (MOT) to a standard MOT from where the cloud is adiabatically transferred in several intermediate steps into a Ioffe-Pritchard type magnetic trap, and a Ti:sapphire laser resonantly pumps the cavity mode. The observations of superradiance in the bad cavity regime of the CARL and at temperatures as high as several $100\mu K$ proved that the gain process underlying superradiant Rayleigh scattering and collective atomic recoil lasing is not based on quantum statistics but on cooperativity.

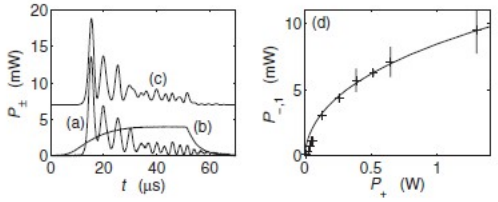

FIG. 2. (a) Measured time evolution of the reverse power P_-. The pump laser power is $P_+ = 4$ W. The cavity is operated at high finesse. The atom number is $N = 1.5 \times 10^6$ and the laser wavelength is $\lambda = 797.3$ nm. Curve (b) marks the time evolution of the recorded pump laser power scaled down by 1000. Curve (c) shows (offset by 7 mW) a numerical simulation of the reverse power using the above parameters (see text). To account for the finite switch-on time of the pump laser power, its experimentally recorded time evolution is plugged into the simulations, where we assume that the pump laser frequency is fixed and resonant to a cavity mode. (d) Measured and calculated (solid line) height $P_{-,1}$ of the first peak as a function of pump power P_+. Here $N = 2.4 \times 10^6$ and $\lambda = 796.1$ nm.

4 Scattering in Bose Einstein Condensates

Now we take ultracold atoms in consideration. Here, the atoms no longer interact with light as point particles, but as quantum-mechanical waves.

The atomic wavefunction $\psi(z,t)$ obeys

$$i\hbar\frac{\partial\psi(z,t)}{\partial t} = -\frac{\hbar^2}{2m}\frac{\partial^2\psi(z,t)}{\partial z^2} - i\hbar g_p(ae^{2ikz} - c.c.)\psi(z,t)$$

The atoms are represented as their quantum mechanical average and optical field becomes

$$\frac{da}{dt} = g_p N\int|\psi|^2 e^{-2ikz}dz - \kappa a + i\delta a$$

In terms of the momentum eigenstates $|n\rangle$, $\psi(z,t) = \sum_n c_n(t)\,|n\rangle$ where $|n\rangle = \frac{1}{\sqrt{2\pi}}e^{2inkz}$, our equations become

$$i\hbar\frac{dc_n}{dt} = (-2\hbar k)^2(-\frac{\hbar^2}{2m})c_n - i\hbar g_p(ac_{n-1} - a^*c_{n+1})$$

$$\frac{da}{dt} = g_p N(\sum_n c_n c_{n-1}^*) - \kappa a + i\delta a$$

The atom-field momentum exchange is no longer continuous and only discrete values of momentum exchange are possible. This model describes classical collective atomic recoil lasing as well as collective Rayleigh scattering behaviour where the simulation is similar to a 2-level atom with momentum states replacing internal states. Also, it is used to explain other "quantum" collective regimes involving at most 2 momentum states at any time. Thus, the equations for ultracold atoms form a fully quantum model and the superradiance measured and the recoiling atomic distribution becomes an area of interest for various other quantum experiments.

4.1 Experimental Realizations

With developments in laser cooling and trapping led to new opportunities for research in light matter interactions for ultracold atoms. One of the first experiments on light matter interactions in a BEC was done by MIT in 1999[5] where an elongated Bose-Einstein condensate ($20\mu m$ diameter, $200\mu m$ length) containing Na atoms prepared in a magnetic trap was exposed to a single off-resonant laser beam(detuned by 1.7 GHz) resulted in the observation of highly directional scattering of light and atoms.

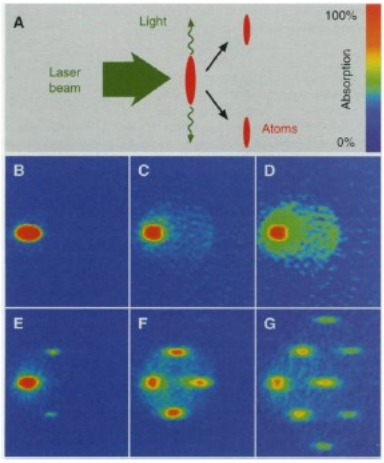

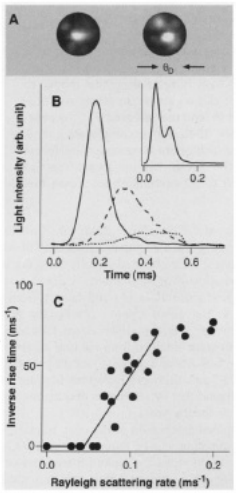

Fig. 3. Observation of directional emission of light. **(A)** The angular pattern of the emitted light along the axial direction showed a few bright spots with an angular width θ_0 ($1/e^2$ diameter) of 107 ± 20 mrad, corresponding to the diffraction-limited angle of an object of ~14 μm in diameter. The images were integrated over the entire duration of the light pulse. **(B)** The temporal evolution of the light intensity showed a strong initial increase characteristic of a stimulated process. For higher laser power, the pulse was shorter and more intense. The laser intensities were 3.8 (solid line), 2.4 (dashed line), and 1.4 (dotted line) mW/cm², and the duration was 550 μs. The inset shows a double peak in the temporal signal when the laser intensity was about 15 mW/cm², which was above the threshold for sequential superradiant scattering. The photomultiplier recorded the light over an angle of 200 mrad around the axial direction. **(C)** The dependence of the inverse initial rise time on the Rayleigh scattering rate shows a threshold for the stimulated process. The solid curve is a straight-line fit.

The light scattered by the atoms interfere constructively in phase-matching direction giving total power as:

$$P = \hbar\omega f_j R \frac{N_{mod}^2}{4}$$

where $f_j = \frac{\sin^2\theta_j}{8\pi/3}\Omega_j$ (θ_j is the angle between incident polarization and direction of emission, phase matching by solid angle $\Omega_j \sim \lambda^2/A$, A is the cross-sectional area of the condensate perpendicular to direction of emission);
$N_{mod} = 2\sqrt{N_0 N_j}$ is the density modulation (N_0 condensate atoms at rest, N_j recoiling atoms with momentum in phase-matching direction); R is the single-atom Rayleigh scattering rate; ω is the frequency of the radiation

Also, it was observed that the momentum distribution of atoms depends on the polarization of the laser beam, i.e., for parallel polarization, atoms followed a dipolar pattern of normal Rayleigh scattering, whereas for perpendicular polarization, the recoiling atoms acted as highly directional beams

propagating at 45deg to the long axis. A quantum-mechanical model yields the result for growth rate of N_j as

$$\dot{N}_j = RN_0 \frac{\sin^2 \theta_j}{8\pi/3} \Omega_j (N_j + 1)$$

It was observed that the interference pattern in the density distribution acts a grating making a self-amplification process where the recoiling atom stimulates the next atom to scatter in the same direction. With the study of an ensemble of atoms in a single quantum state, they concluded that the long coherence time of a BEC resulted in superradiance based on coherent external motion.

Building on the experiment in MIT, researchers at Utrecht University[15] observed a second scattering process in which the recoil of the atom is directed backwards at an angle of ± 135 deg w.r.t. the incoming laser, but the photon from the endfire mode gets scattered back into the laser creating an energy deficit equivalent to $4E_r$ (recoil energy). Thus, they used another laser to drive the backward-scattering resonantly and the frequency difference between the two lasers control the ratio of the number of forward and backward scattered atoms. Here a BEC ($40\mu m$ diameter, $1mm$ length) containing $1.2x10^8$ Na atoms in $F_g = 1$, $M_g = -1$ ground state is trapped in a cloverleaf magnetic trap with frequencies $\nu_z = 4Hz$(axial)$\nu_\rho = 99Hz$(radial), at 450 nK and illuminated by two lasers of perpendicular polarization with joint detuning ranging from -5 GHz to +5 GHz.

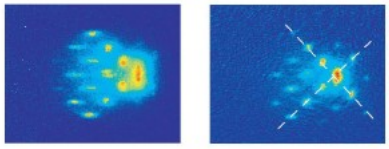

FIG. 2: The results for superradiant scattering using a pulse length of 100 μs, an intensity of 1.6 mW/cm^2 and a detuning of -3 GHz, where the largest cloud is the original condensate. The picture on the left shows the momentum distribution after illumination by a laser beam incident from the right with one frequency. The picture on the right shows the results after illumination with two laser beams incident from the right with a frequency difference of 100 kHz.

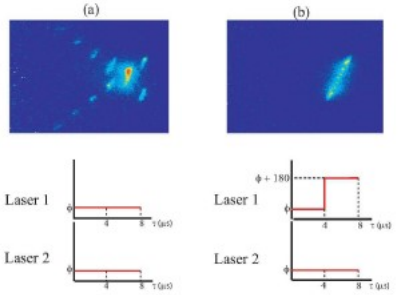

FIG. 6: (a) The scattering pattern after applying two laser pulses for 8 μs, where the phase ϕ of both lasers is kept constant during the process. (b) The scattering pattern for the same settings, but now the phase ϕ of one of the laser pulses is changed by 180° halfway during the pulse. The laser pulse has a detuning of +3 GHz and an intensity of 20 mW/cm^2.

They observed that the scattering of atoms in the forward and backward directions were strongly correlated which was evident from the temporal behaviour of the outcoupling of the forward and backward scattered atoms on resonance.

Moreover, it was observed that the whole outcoupling can be reversed by reversing the phase of one laser at halfway through the pulse.

4.2 Trapped Bose-Einstein condensates

With an advent of the realization of superradiant Rayleigh scattering experimentally, an increased interest in light matter interactions in a BEC takes place. This interest varies over the the environment of the interaction and study of optical evolution i.e. the nature of scattering of light and the atomic distribution i.e. the atom state evolution for these interactions, becomes significant. We take 2 major cases into consideration, one for **trapped Bose-Einstein condensates in a cavity**, and the other for **free BEC gas in quantum degeneracy**.
Following this, researchers at Georgia Institute of Technology developed a model for these interactions in 2000[9], for trapped BECs. Their model consists of the optical evolution according to the light-matter interactions for different atomic field conditions and found that the scattered light intensities can exhibit both oscillatory as well as exponential behaviour depending on densities, temperatures, pump pulse characteristics and geometric shapes of trapped gas samples.

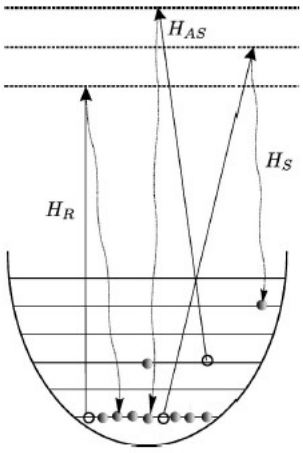

FIG. 2. The diagram for Rayleigh, Raman Stokes, and anti-Stokes scattering among the motional states of trapped atoms. The solid lines denote pump photons while dotted curved lines are for scattered photons. Solid dots denote the presence of an atom, and hollow dots denote the absence of atoms due to scattering out of certain motional states.

They identified the major scattering events as elastic Rayleigh scattering and inelastic Raman scattering (Stokes and Anti-Stokes equations) and their Hamiltonian takes the form:

$$H = H_0 + H_R + H_{AS} + H_S$$

$$H_0 = \sum_n E_n c_n^\dagger c_n + \int d\vec{k}\omega_k b_{\vec{k}}^\dagger b_{\vec{k}}$$

$$H_R = \sum_n \int d\vec{k} g^*(\vec{k},t)\eta_{n,n}(\vec{k}-\vec{k_0})c_n^\dagger b_{\vec{k}}^\dagger c_n + H.c.$$

$$H_{AS} = \sum_n \sum_{m\in(E_m>E_n)} \int d\vec{k} g^*(\vec{k},t)\eta_{n,n}(\vec{k}-\vec{k_0})c_n^\dagger b_{\vec{k}}^\dagger c_m + H.c.$$

$$H_S = \sum_n \sum_{m\in(E_m<E_n)} \int d\vec{k} g^*(\vec{k},t)\eta_{n,n}(\vec{k}-\vec{k_0})c_n^\dagger b_{\vec{k}}^\dagger c_m + H.c.$$

where effective coupling constant $g(\vec{k},t) = \Omega_0 T(\gamma_0 t) g(\vec{k})/2\Delta$ (Ω_0 is the Rabi frequency, $T(\gamma_0 t)$ is the envelope function and $\Delta = \omega_A - \omega_0$ is the detuning)
$b_{\vec{k}}^\dagger, b_{\vec{k}}$ are photon creation and annihiliation operators, $c_n^\dagger, c_n$ are atomic creation and annihiliation operators, pump pulse has $\vec{k_0}$ wave vector and $\vec{\epsilon_k}$ polarization, and motional state dipole transition moment is described with displacement operator as $\eta_{n,m}(\vec{k}) = \langle n|\, exp(i\vec{k}\cdot\vec{r})\,|m\rangle$

Some of their observations include - At small angles of incidence and low temperatures, coherent Rayleigh scattering is dominant but Raman scattering(especially Stokes term) can be made dominating by elongating the current trap. At large angles - Raman scattering(short pulse Stokes) is the dominant process and it carries the information of condensate number fluctuations directly. An effect of using this is creation of strongly couply atomic side modes giving rise to sequential recoiling atoms in turn getting multiple superradiant peaks describing it in terms of a cascading lattice structure.

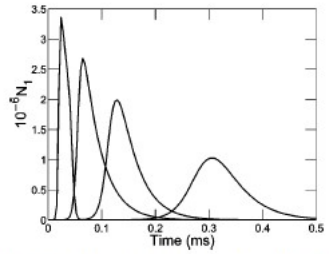

FIG. 15. The evolution of the first side mode(s) within a Markov approximation for scattered light.

Their study presented a thorough investigation of the superradiant light scattering for trapped BECs. They also compared a theoretical Markov approximation with an experimental non- Markovian description(multiple superradiant peaks) for the light scattering observations, creating a general network for light scattering studies for trapped BECs.

With realizations in matter wave superradiance and phase-coherent amplification of matter waves, an illustration of practical use of light scattering in a BEC was proposed in 2000[8] to use spontaneoud Raman scattering from an optically driven Bose-Einstein condensate to produce maximally entangled atom-photon pairs which is very useful for applications in quantum-information as the atom can be easily trapped and manipulated while the photon can be easily transmitted.

They modeled for a sodium BEC to produce Raman scattering to make maximally entangled atom-photon pairs and the photodetectors detect shorter wavelength photons to be entangled with atoms in F = 1 state, with maximally entangled state as $|\psi_e\rangle = \frac{1}{\sqrt{2}}(|\sigma_+, -1\rangle + |\sigma_-, 1\rangle)$ and applying that to present technology found that the yield for entangled atom-photon pairs would be around 0.005 for +ve and -ve directions and using same parameters as the 1999 paper, entanglement is produced at a rate of 10^5 entangled pairs in 100 s.

Pertaining to the light matter interactions, the study of atom state evolution and collapse becomes apparent and the change in atomic state during the light scattering event in a cavity was modelled by researchers at Harvard and Innsbruck in 2011[7].

Assuming the probe, cavity and lattice satisfy the condition of the diffraction maximum for light scattering, the probability to find the atom number 0¡z¡N in the lattice region of K sites is given simply:

$$p(z, m, t) = z^{2m} e^{-z^2 \tau} p_0(z) / \tilde{F}^2(m, \tau)$$

where $\tilde{F}^2(m, \tau) = \sum z^{2m} e^{-z^2 \tau} p_0(z)$, $\tau = 2|C|^2 \kappa t, C = iU_1 0 a_0 / (i\Delta_p - \kappa)$,

$p_0(z)$ is the initial distribution and $\tilde{F}$ proves the normalization. The light amplitude corresponding to the atom number z is $\alpha_z = C_z$.

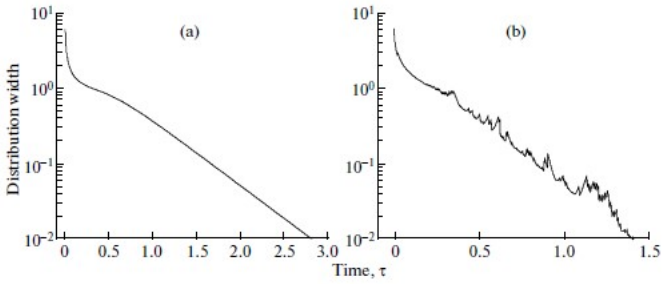

Fig. 1. Width of the atom number distribution function during the photodetection. Decreasing width corresponds to the atom number squeezing. At the initial stage, the shrinking is as $1/\sqrt{\tau}$, while at the final stage the shrinking is exponential. (a) Quantum trajectory without quantum jumps; (b) quantum trajectory with quantum jumps. Photodetection is at the diffraction minimum. Total number of atoms $N = 100$, $K = M = 100$ sites.

Here, the unitary evolution of the light-matter quantum state showed the non-trivial phase dependence, quadratic in the atom number. More importantly, we get to understand the square root dependence for the initial stage of state collapse and exponential shrinking in the final stage of state collapse due to the discrete nature of atom number distribution.

Now, seeing quantum trapping with great potential, [2]Oxford university researchers theorize an entangled system for atoms in a quantum many-body correlated phase of matter with the properties of light where a quantum optical lattice allows the superposition of structured squeezed coherent states of light entangled with matter(interplay between optical cavity long range interactions and atomic short-range processes).

They formed an effective master equation for quantum optics for BECs trapped in optical lattice (taking into account all the light matter behaviour and their interactions, quadratures of light, squeezing of atomic states as well as coupling at lattice sites)is given by:

$$\frac{d\tilde{\rho}}{dt} = -\frac{i}{\hbar}[H_{eff}, \tilde{\rho}] + \frac{g_{eff}\kappa}{\Delta_c}(2\hat{G}^\dagger\tilde{\rho}\hat{G} + [\hat{G}^\dagger\hat{G}, \tilde{\rho}]_+)$$

,

$$\tilde{\rho} = \sum_{\varphi_q,\varphi_l} p_{q,l}\beta_{\varphi_l}\beta_{\varphi_l} \left|\tilde{\alpha_{\varphi_q}}, \xi_{\varphi_q}\right\rangle_a |\varphi_q\rangle_b \, {}_b\langle\varphi_l|_a \langle\xi_{\varphi_l}, \tilde{\alpha_{\varphi_l}}|$$

where $\tilde{\rho}$ is the density matrix, $[.,.]_+$ is the anti-commutator and $p_{q,l}$ are the matter probabilities that describe either a pure or mixed state; and the second term is the effective Liouvillian which explains dissipation.

This equation can be used to create global structured dissipation channels and measurement induced projection and state design of non-trivial quantum correlated states.

Thus, a quantum optical lattice offers a generalized class of states that are a non trivial superposition of structured squeezed coherent states of light entangled with matter as the induced long-range processes and ordinary short-range atomic processes lead to modification of effective Hamiltonian. The quantum parameters of light like photon number and quadratures light are accessed by the quantum many-body matter states and light contain information of matter- field coherences, density patterns of matter and light-matter quantum correlations(properties of strongly correlated phases of matter get imprinted on the quantum properties of light).

With representation of ultracold atoms in optical lattices, the structural properties of crystalline solids become an area of interest and hence bragg scattering for the lattice is measured and thus performed by Bragg spectroscopy by measuring the scattered photons which carry the signatures of Mott insulator and superfluid quantum state[12] (as the latteice atomic state function evolves though the Mott insulator-superfluid phase transition).

They study the self-organisation behaviour of light as it couples to the atomic transition to form an atomic crystalline structure and is then diffracted by the same. They formulate the transition to Mott insulator phase as all lattice points in the optical lattice gets equally occupied, which transitions into a superfluid state according to the quantum fluctuations in the number of atoms per site (Here, the laser excites the atom very weakly to obtain the lowest order atom-photon interaction) and then observe a single peak at each Bragg angle (as expected in the weakly interacting superfluid phase), which is further used to plot the Bragg signal intensiy as a function of the optical lattice depth.

When Bragg spectroscopy is performed with light scattering, the photon recoil provides additional atomic site-to-site hopping which interferes with ordinary matter-wave tunneling and affects the photonic-scattering cross section, with the use of a weak probe and far-off resonance from both the frequencies of atoms and lattice beam. Thus, Bragg spectroscopy modifies the atomic system by scattered photons imparting recoil perturbing the state of the atomic gas thereby affecting spectroscopic signal by interfering with ordinary tunneling between sites and there is a need for nondemolition type measurement methods.

Coming back to entanglement, an interesting experiment for entanglement between stationary systems at remote locations was performed which has great potential for creating quantum networks[10]. Here, the approach

is remote entanglement between single atom and BEC where a single atom in a cavity generates a photon which gets stored in a BEC and an entanglement relation is built between the atom and BEC for a particular time($100\mu s$ here). After arbitrary delays, the relation changes to photon-photon entanglement and the measurement of both the photon's polarizations give the entanglement relation. Experiment - A single photon pulse was made to emit from a single ^{87}Rb atom in a high finesse optical cavity which creates the entangled atom-photon state

$$|\psi_{at\otimes ph}\rangle = (|1,1\rangle \otimes |L\rangle - |1,-1\rangle \otimes |R\rangle)/\sqrt{2}$$

($0.45\mu s$ single photon pulse) which was transported 30 m to be absorbed in an ^{87}Rb BEC using Raman transfer. This establishes the entangled atom-state-BEC state

$$|\psi_{at\otimes BEC}\rangle = (|1,1\rangle \otimes |2,-1\rangle - |1,-1\rangle \otimes |2,1\rangle)/\sqrt{2}$$

(BEC serves a quantum memory for one particle of Einstein-Podolsky-Rosen pair). After the matter matter entanglement, a single photon is retrieved from the BEC and generation of a second photon in the cavity produces the maximally entangled two-photon singlet pulse

$$|\psi_{ph\otimes ph}\rangle = (|R\rangle \otimes |L\rangle - |L\rangle \otimes |R\rangle)/\sqrt{2}$$

. They demonstrated that remote entanglement of a single atom and a BEC has the potential to become deterministic, which opens up opportunities in quantum logic gates based on magnon-magnon interaction in the BEC.

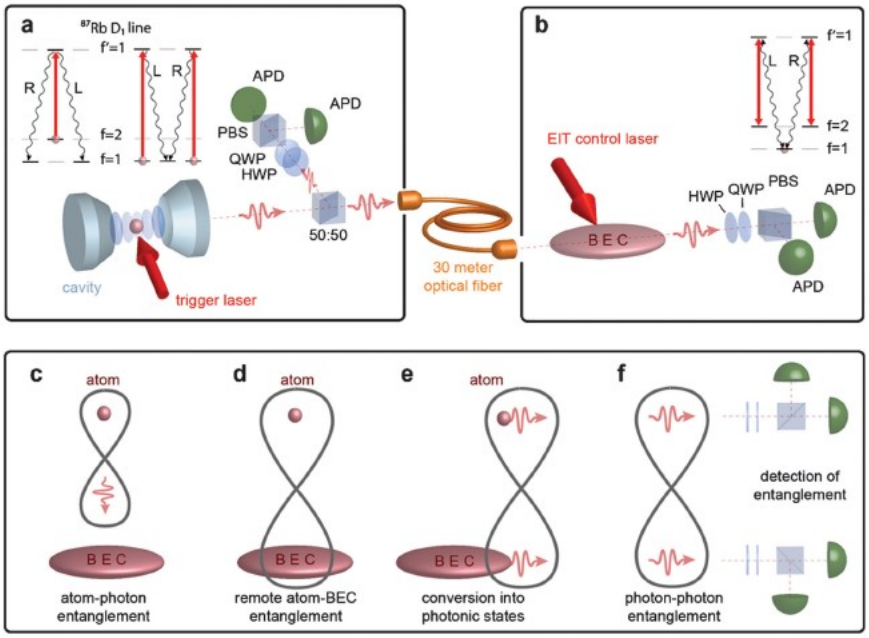

FIG. 1 (color). Scheme of the experiment. (a) A single atom inside an optical cavity serves as a source for polarization-entangled pairs of single photons. After impinging on a 50:50 beam splitter, the photon polarization can either be measured immediately or the photon can be transported in an optical fiber to a different laboratory (b), where a BEC serves as an EIT-type quantum memory. After storage, the photon is retrieved and its polarization is measured. Some optical components, such as mode-filtering fiber, filter cavity, etc., are not shown here. (c) The experimental sequence begins with a trigger pulse which illuminates the single atom to generate a single photon. This process creates a maximally entangled Bell state of the photon polarization and the atomic spin state; see Eq. (1). (d) After transport in an optical fiber, the single photon is stored as a spin-wave excitation in the BEC. This establishes remote atom-BEC entanglement, see Eq. (2). (e) After arbitrary delays, which can be chosen independently for each atomic system, the matter-matter entanglement is converted into photon-photon entanglement, see Eq. (3). (f) Finally, the polarizations of both photons are measured.

4.3 Free Gaseous Bose-Einstein condensates in quantum degeneracy

With the extension of the study of light matter interactions in a BEC, the study for coherent joint propagation of light and matter wave in a BEC as a degenerate quantum gas becomes emminent, and thus researchers in St-Peterburg formulate the theory of light scattering from a BEC in the state of quantum degeneracy, where the BEC is considered in the framework of the Gross- Pitaevskii model and use self-consistent Green's function analysis for optical excitation description. [4]The photon scattering here is based on the formalism of the T-matrix:

$$\hat{T}(E) = \hat{V} + \hat{V}\frac{1}{E - \hat{H}}\hat{V}$$

and the scattering amplitude for a single particle excitation in the BEC based on these elements gives(using Green's function):

$$T_{fi}(E) = \frac{2\pi\hbar(\omega_{k'}\omega_k)^1/2}{\mathcal{V}} \int\int d^3r'd^3r \sum_{n',n} (de')^*_{n',0}(de)_{0n} e^{-k'r'+ikr}\Xi^*(r')\Xi(r)$$

$$\mathbf{x}\frac{-i}{\hbar}\int_0^{\inf} dt e^{\frac{i}{\hbar}(E-E_0^N+i0)t} iG_{n',n}(r',t;r,0)$$

where E_0^N is the initial energy of the condensate consisting of N particles and

$$iG_{n',n}(r',t;r,0) = \langle BEC|\, T\psi_{n'}(r';t')\psi^\dagger_n(r;t)\,|BEC\rangle^{N-1}$$

and with standard definitions, the polariton propagator obeys the following:

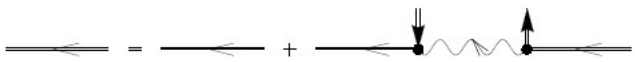

where double line represents all interaction processes, vertical arrows are ordering parameters forming self-energy responsible for coherent conversion of excitation, wavy line are the free dynamics The incomplete atomic propagator obeys Dyson-type equation:

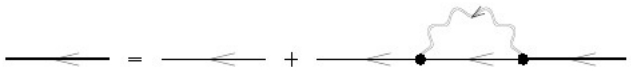

which together makes the field propagator equation:

They modeled this behaviour for longitudinal and tranverse light wave with Rb D2-line for $\lambda = 780nm$ which gave the results of fast propagation of the

polariton through the sample (superfluidity) and strong coherent scattering from sample boundaries from

$$G_{\parallel}(k,\omega) = \left[\omega - \omega_0 - \frac{\hbar k^2}{2m} - \frac{8\pi n_0 d_0^2}{3\hbar} + \frac{i\sqrt{\epsilon(\omega)\gamma}}{2}\right]^{-1}$$

$$G_{\perp}(k,\omega) = \left[\omega - \omega_0 - \frac{\hbar k^2}{2m} + \frac{4\pi n_0 d_0^2}{3\hbar} + \frac{i\sqrt{\epsilon(\omega_E)\gamma}}{2} - \frac{4\pi n_0 d_0^2 \omega^2}{\hbar(\omega^2 - c^2k^2)}\right]^{-1}$$

They observed that a superposed state of field and matter i.e. polariton wave is formed when light passes through a degenerate atomic BEC gas which displays strong coherent scattering from sample edges. Furthermore, they propose using this property to develop optomechanical quantum interface schemes between the non-classical light and condensate (macroscopic quantum property - superfluidity).

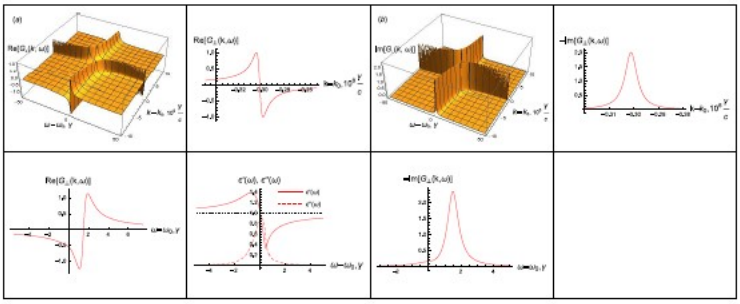

Figure 1. The transverse component of the polariton propagator $G_{\perp}(k,\omega)$ plotted for the density $n_0(\lambda_0/2\pi)^3 = 0.05$, where $\lambda_0 = 780\,\text{nm}$ is the radiation wavelength at atomic resonance: (a) Real part and (b) Imaginary part. Other graphs show the resolved spectral profiles, taken at the edges of three-dimensional plots (a) and (b), and the dielectric permittivity of the sample $\epsilon(\omega) = \epsilon'(\omega) + i\epsilon''(\omega)$ calculated in [16].

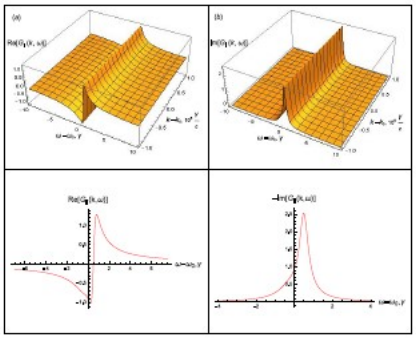

Figure 2. Same as in Fig. 1 but for longitudinal component of the polariton propagator $G_{\parallel}(k,\omega)$.

With the incident photon being influenced by the presence of incoherent scattering channels, more insight into this model was needed, and the propagator tracking by Green's function is further studied and in 2018[11], researchers took into account the incoherent channels for the joint coherent dynamics of the optical excitation and compared the solution of polariton dynamics in the outgoing channel with the conventional macroscopic Maxwell theory of light scattering from a nondegerate atomic sample. They incorporated the incoherent losses and the dielectric permittivity of the condensate by the closed scattering equation to get the complete polariton propagator:

$$G_{\parallel}(p,E) = \hbar \left[E - E_n - \frac{p^2}{2m_A} - \frac{8\pi}{3} n_0 d_0^2 + \frac{i\hbar}{2}\sqrt{\epsilon(\omega_E)\gamma} \right]^{-1}$$

$$G_{\perp}(p,E) = \hbar \left[E - E_n - \frac{p^2}{2m_A} + \frac{4\pi}{3} n_0 d_0^2 + \frac{i\hbar}{2}\sqrt{\epsilon(\omega_E)\gamma} - \frac{4\pi n_0 d_0^2 \omega_E^2}{(\omega_E^2 - c^2p^2/\hbar^2)} \right]^{-1}$$

where these represent the longitudinal and transverse components of the polariton propagator. These equations are pretty similar to the equations derived earlier but the crucial difference here is that the atomic medium represents a coherent matter wave leading to rejection of classical representation. The quantum degenerate atomic system exists in a steady state and can be associated with the stationary solution of the Gross-Pitaevskii equation as discussed previously but here we observe a significant difference once the BEC is fractured into a number of interfering matter wave fragments and the scattering process evolves towards the conditions of Bragg diffraction which is a specific case since the oscillating matter pattern is mostly sensitive to the relative speed of the fragments.

[6]Another interesting phenomenon for free space BEC- light interactions is the formation of crystalline states of light and atoms where stationary periodic configuration particles try to maximize scattering of light and minimize atomic potential energy by breaking a continuous translational symmetry. This periodic pattern formation for an atomic BEC in free space was produced by far off-resonant counterpropagating and noninterfering lasers of orthogonal polarization.

Here, a mirror symmetric and translation invariant setup in which an elongated BEC longitudinally illuminated by two counterpropagating Gaussian beams far detuned from any atomic resonance, which gives a supersolid BEC trapped in an emerging optical lattice that displays collective phononic excitations. It was also observed that these states are unstable above a particular threshold as small density fluctuations lead to backscattering in turn

creating a feedback for the fluctuations and this critical driving intensity was found out to be

$$I_C^{L,R} = \frac{cE_{rec}N}{\lambda_0 A}\frac{1}{\zeta^2} = cE_{rec}\frac{\epsilon_0^2}{\alpha^2}\frac{1}{n}\frac{\lambda_0}{L}$$

where recoil energy $E_{rec} = \hbar\omega_{rec} = \hbar^2 k_0^2/(2m)$

Now, after developing the conditions for creating stationary crystalline states, the dynamics of these states were studied and compared to standard crossed beam dipole traps and it was found that onw has to simply adapt and control the polarizations of the trapping lasers and choose suitable detunings. This ordering process can be observed directly by looking at the reflected light from the condensate and this provides a very good way for nondestructive measurement of real-time monitoring of the dynamics of the BEC structure, opening up opportunities in quantum simulations with ultracold atoms.

An experiment realization of the light scattering experiments for degenerate gas was done as a thesis project by Salim Balik in 2009[1] where high density ultracold ^{87}Rb gas was perpared to observe Andersonian localization of light, i.e. localization of electrons in a disordered medium, which is why they perform a transition from F=2 to F=3 fock state for ultracold ^{87}Rb gas which lies near the localization limit.

Here, He-Ne laser, and CO_2 laser (to make CO_2 dipole traps) are used as the pump lasers to trap the BEC for the experiment. Also 3 acousto-optic modulators are used - Magneto-optical trap AOM, Probe AOM at fixed frequencies and AOM1 that varies, for making the transition of F=2 to F'=3 hyperfine state for ^{87}Rb gas, and the temperature scale used was from 21 to $65\mu K$, then QUEST analysis was performed.

As a result of the experiment, it was observed that even though saturation intensity was $\sim 1.7mW/cm^2$, only a linear increase was observed in signal up to $12mW/cm^2$ probe laser intensity (atoms are deep inside and coherent beam intensity diminishes by the time it reaches those atoms).

To investigate light scattering from high density and ultracold ^{87}Rb gas and look for experimental signatures of localization of light (absence of diffusion of waves in a disordered medium), ultracold high density Rb vapor was optically pumped, it was observed that the light scattering depends on the hyperfine optical pumping, detuning from optical resonance and the density of the sample. Also no long time decays of the fluorescence signal was observed since it was measured that the light had minimal penetration into the sample for the maximum density sample. Thus low density samples might probably give better results. Also, they propose more research in light

localization in ultracold atomic mediums as they say that theory preceeds the experiments in this field.

5 Conclusions and future prospects

With the study of the light-matter interactions in a Bose-Einstein condensate, we describe peculiar results of these interactions which then depends on the conditions of the experiments. This provides us with interesting processes of developing quantum interface protocols between light and matter subsystems. We described optical field interactions with an atom and determine the changes in optical field as well as atomic distribution. We know that light travels significantly slowly in a Bose-Einstein condensate because of the interactions of light with the atoms which gives us an extensive study about the light scattering events in the BEC and about the properties of the BEC. We construct semiclassical as well as fully quantum model for the interactions and describe the theoretical and practical work done in this area of interest. With superradiant scattering and coherent matter wave growth, there comes the potential of creating many-particle entanglement by controling the superradiant backward scattering process. Adding to this, the interactions are widely different for trapped BECs and free space BECs which broadens the area of their applications. We studied the nature of light scattering and atom state growth and collapse for trapped BECs and see the potential in applications of practical optical devices by creating tunable coherent light sources. Moreover, an atom cloud can act as a gain medium for both matter waves and light giving rise to matter wave amplification, therby producing an atom laser by buildup of matter field and wave field in an atom cavity. We also realize the nature of light matter interactions for free space BECs and see the potential in optomechanical quantum interface schemes between the non-classical light and condensate by showing superfluidity. Additionally, these interactions give rise to entanglements of atom-BEC, atom-photon and photon-photon which can eventually lead to tremendous applications, one of which is - the BEC can be easily modified in a lattice and an entangled photon can be easily transmitted which can carry the information related to the BEC. An atom-BEC entanglement lead to creation of quantum logic gates based on magnon-magnon interactions in the BEC. The creation of sequential generation of entangled multiqubit states can be used to create a quantum network of several entangled BECs. With such great potential of light-matter interactions for a Bose-Einstein condensate, there is a great need for more research (theoretical and experi-

mental) for direct applications in quantum information networks.

6 Acknowledgement

I owe a great debt of gratitude to my advisor Dr. Gian-Luca Oppo for giving me the chance to work with him. This essay could not have been completed without his continuous support, guidance and patience. I have learned a great deal as he was always there offering guidance and thoughtful training. I also would like to thank him for Dr. A Daley and Dr. A M Yao for their help in data acquisition and making me understand it. I am confident that they will move the research forward and be successful.

References

[1] Salim Balik. *Light scattering in ultracold high density rubidium vapor*. Old Dominion University, 2009.

[2] Santiago F Caballero-Benitez and Igor B Mekhov. "Quantum properties of light scattered from structured many-body phases of ultracold atoms in quantum optical lattices". In: *New Journal of Physics* 17.12 (2015), p. 123023.

[3] Robert H Dicke. "Coherence in spontaneous radiation processes". In: *Physical review* 93.1 (1954), p. 99.

[4] VM Ezhova, LV Gerasimov, and DV Kupriyanov. "On a theory of light scattering from a Bose-Einstein condensate". In: *Journal of Physics: Conference Series*. Vol. 769. 1. IOP Publishing. 2016, p. 012045.

[5] S Inouye et al. "Superradiant Rayleigh scattering from a Bose-Einstein condensate". In: *Science* 285.5427 (1999), pp. 571–574.

[6] Matthias Lettner et al. "Remote entanglement between a single atom and a Bose-Einstein condensate". In: *Physical Review Letters* 106.21 (2011), p. 210503.

[7] Igor B Mekhov and Helmut Ritsch. "Atom state evolution and collapse in ultracold gases during light scattering into a cavity". In: *Laser Physics* 21.8 (2011), pp. 1486–1490.

[8] MG Moore and P Meystre. "Generating entangled atom-photon pairs from Bose-Einstein condensates". In: *Physical review letters* 85.24 (2000), p. 5026.

[9] Özgür E Müstecaplioğlu and L You. "Superradiant light scattering from trapped Bose-Einstein condensates". In: *Physical Review A* 62.6 (2000), p. 063615.

[10] Stefan Ostermann, Francesco Piazza, and Helmut Ritsch. "Spontaneous crystallization of light and ultracold atoms". In: *Physical Review X* 6.2 (2016), p. 021026.

[11] VM Porozova et al. "Light scattering from an atomic gas under conditions of quantum degeneracy". In: *Physical Review A* 97.5 (2018), p. 053805.

[12] Stefan Rist, Chiara Menotti, and Giovanna Morigi. "Light scattering by ultracold atoms in an optical lattice". In: *Physical Review A* 81.1 (2010), p. 013404.

[13] N Skribanowitz et al. "Observation of Dicke superradiance in optically pumped HF gas". In: *Physical Review Letters* 30.8 (1973), p. 309.

[14] S Slama et al. "Superradiant Rayleigh scattering and collective atomic recoil lasing in a ring cavity". In: *Physical review letters* 98.5 (2007), p. 053603.

[15] KMR van der Stam et al. "Resonant superradiant backward-scattering as a source for many-particle entanglement". In: *arXiv preprint arXiv:0707.1465* (2007).